Experimental-numerical approach to efficient TTT-generation for simulation of phase transformations in thermomechanical forming processes

Experimental-numerical approach to efficient TTT-generation for simulation of phase transformations in thermomechanical forming processes

B.-A. Behrens, A. Chugreev, C. Kock[1)]

IFUM – Institut für Umformtechnik und Umformmaschinen, Leibniz Universität Hannover, An der Universität 2, Garbsen 30823, Germany

[1)] E-mail: kock@ifum.uni-hannover.de, phone +49 511 762 2161

Abstract. Residual stresses in components are an important issue in most manufacturing processes, as they influence the performance of the final part. Regarding hot forming processes there is a great potential of defining a targeted residual stress state, due to numerous adjustment parameters like deformation state or temperature profile. In order to ensure appropriate numerical modelling of resulting residual stresses in a thermomechanical process, comprehensive material data regarding phase transformation are required. This paper presents an experimental-numerical procedure to efficiently determine time-temperature-transformation diagrams for cooling simulations after hot forming. The transformation behaviour of the steel alloys 42CrMo4 and 100Cr6 is determined by experiments as well as FE-simulations. Finally, the simulation model is validated by dilatometric experiments and metallographic investigations.

1 Introduction

In forming processes, the arising residual stresses influence the material behaviour during and after manufacturing as well as the performance of the final component [1]. This calls for a thorough consideration and evaluation of the mentioned residual stresses. Hot forming, in particular, represents not only a great challenge for numerical prediction of the resulting stress states but also a high potential for the targeted adjustment of residual stresses due to numerous influencing factors resulting from the thermomechanical process [2, 3]. During such a process, the degree of deformation after hot forming in combination with the temperature-time profile experienced by the component have an important influence [4]. In general, the polymorphic transformation behaviour of the microstructure in steel alloys is described by continuous-cooling-transformation (CCT) diagrams and time-temperature-transformation (TTT) diagrams. Thereby, CCT describe the transformation behaviour of the material during continuous cooling, whereas TTT represent the transformation behaviour after quenching and subsequent holding at a certain test temperature [5]. Such diagrams are either provided by steel manufacturers or listed, for example, in compendia for heat treatment [6]. Furthermore it is possible to calculate CCT- and TTT-diagrams on the basis of the chemical composition of the steel alloys with the software JMatPro from Sente Software [7] using the empirical equations from the work of *Kirkaldy et al.* [8] and *Li et al* [9]. However, each of these diagrams is strongly dependent on the experimental boundary conditions. For example, *Schulze et al.* [10] investigated the influence of grain growth on the transformation behaviour of a 42CrMo4 steel alloy due to heating strategy, austenitisation temperature and holding time. Another important influence on the phase transformations is the deformation state

applied before cooling, which is why deformation-dependent diagrams D-CCT-diagrams and D-TTT-diagrams are recorded in literature [11, 12]. For these reasons, it is important to always use transformation diagrams specifically for the process under consideration. For numerical description of phase transformations the Koistinen-Marburger equation is widely used for diffusion-free transformations and the Johnson-Mehl-Avrami equation for diffusion-controlled transformations respectively [13]. However, these two approaches are valid only for isothermal processes, hence commercial FE-solvers like MSC.Marc require isothermal TTT-diagrams for the residual stress calculations by means of phase transformations. The experimental determination of the isothermal TTT-diagrams is very challenging, especially since they are costly and time-consuming due to the long durations of the tests. Besides phase transformations under isothermal conditions are hardly to detect by dilatation measurements. Furthermore, it is challenging to generate sufficiently high cooling rates of more than 175 K/s [14] with the quenching gases helium or nitrogen, to prevent that transformations have already taken place before the testing temperature has been reached [9, 15]. Therefore, some authors have developed mathematical approaches to calculate TTT- from CCT-diagrams [16, 17]. For the numerical investigations of residual stresses it is necessary to implement accurate information about the microstructural transformation process into the FE-software. Therefore, the aim of this work is to determine TTT-diagrams of the steel alloys 42CrMo4 and 100Cr6 with a time and cost efficient as well as precise experimental-numerical approach.

2 Investigation on phase transformation behaviour of steel alloys 42CrMo4 and 100Cr6

As explained in the introduction, there are some restrictions of getting TTT-diagrams directly from experiments. Therefore, this paper presents an approach for the determination of TTT by combination of modern software as well as the established standardised experiments. In the first step CCT-diagrams were calculated by JMatPro based on the chemical composition of the alloys (table 1).

Table 1: Chemical composition of steel alloys 42CrMo4 and 100Cr6 according to international standards [18, 19] used for material data generation with JMatPro.

	C	**Si**	**Mn**	**P**	**S**	**Cr**	**Mo**	**Fe**
42CrMo4	0.42	0.25	0.75	0.025	0.035	1.10	0.22	balance
100Cr6	0.99	0.25	0.35	0.025	0.015	1.475	0.10	balance

Due to batch fluctuations of investigated materials and partial shortcomings of the empirical methods in JMatPro, an experimental fitting of the calculated diagrams by experiments was necessary. Subsequently, the software tool "TTT-CCT-diagram generator" of Transvalor was used to determine the TTT- from the CCT-diagram. The determined TTT were implemented in the Software Simufact Forming 15 to simulate the experimental CCT tests. Finally, by means of the length-change-temperature-profiles and metallographic investigations the simulations were calibrated and validated.

2.1 Experimental determination of continuous cooling transformation diagrams

The experimental CCT-tests were carried out and evaluated at the Institute of Forming Technology and Machines based on the specifications of the "Deutsche Stahl-Eisen-Prüfblätter" SEP 1680 and SEP 1681 [20, 21] at the quenching-deformation dilatometer system DIL 805A/D+T (Co. TA Instruments Inc.). Cylinders with a diameter of 4 mm and a height of 10 mm were examined. The samples were first heated inductively with a heating rate of 50 K/s to the austenitising temperature of 1050 °C followed by a 10 minutes soaking time. Subsequently a cooling phase of 30 seconds to 950 °C takes place. In case of the deformation-dependent CCT-test, the specimens were upset to a degree of deformation of φ=0.6 at a temperature 950 °C and a strain rate of 1 s^{-1}. Afterwards the specimens were linearly cooled by the medium nitrogen. The investigated cooling rates together with the resulting hardness values H are listed in table 2. The obtained results were used to calibrate the CCT-diagrams calculated with JMatPro. Figure 1 shows the CCT-diagrams with and without a previous deformation for both materials. For the alloy 42CrMo4 the formation of ferritic (F), pearlitic (P), bainitic (B) and martensitic (M) phase fractions from the initial austenitic (A) phase was observed.

Table 2: Hardness values of the specimens from experimental CCT-tests.

42CrMo4							
$\dot{\vartheta}$ **[K/s]**	30	6	3	1	0.3	0.15	0.07
H(φ=0) | H(φ=0.6) [HV1]	667|710	647|670	455|456	336|328	317|310	307|272	270|235
100Cr6							
$\dot{\vartheta}$ **[K/s]**	30	5	2.5	1	0.5	0.15	-
H(φ=0) | H(φ=0.6) [HV1]	842|815	832|707	749|486	495|442	425|396	407|366	-

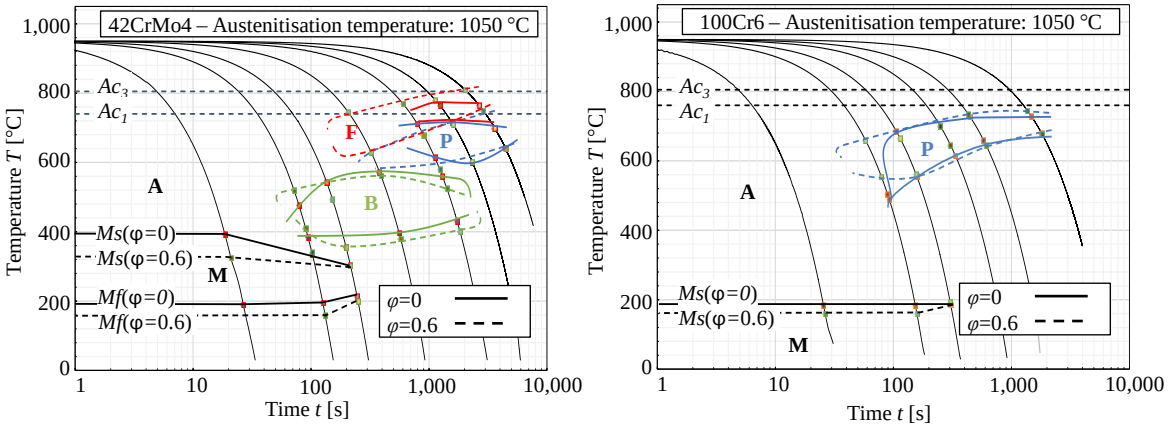

Figure 1: CCT-diagrams for the materials 42CrMo4 (left) and 100Cr6 (right) with and without deformation and an austenitising temperature of 1050 °C.

Obviously, the plastic deformation causes a decrease of the martensite-start-temperature Ms as well as the martensite-finish-temperature Mf. Furthermore, previous deformation influences the ferrite area, which is extended to lower times and temperatures. For the specimens from steel alloy 100Cr6 only the pearlitic and martensitic microstructural phases were observed. Firstly, the steel has a relatively low critical cooling rate (between $\dot{\vartheta}_{crit}$=2.5 K/s and 5 K/s) due to its high carbon content. Secondly, the bainite formation is prevented by means of the high percentage of the carbide former chromium. Thus, before a bainitic transformation can take place, all austenite grains are transformed into either martensite or pearlite grains at a corresponding cooling rate. Due to the finer grain after forming of the specimens, a shift of the pearlite area to lower times was observed. Furthermore, a reduction of Ms in the case of deformed specimens was detected for the specimen from 100Cr6 alloy. However, an Mf could not be determined since the martensitic transformation was not yet completed even at room temperature. Therefore, the samples have to be cooled further below room temperature. As evidence for the experimental CCT-tests all samples were metallographically examined and the most interesting ones are exemplarily shown in figure 2. The steel 42CrMo4 shows the formation of pure bainite in CCT-test with the cooling rate $\dot{\vartheta}$=1 K/s without previous deformation (figure 2a). In case of the CCT-test with $\dot{\vartheta}$=1 K/s and a previous deformation, ferritic and pearlitic phases are formed (figure 2b). Regarding the specimen from 100Cr6, at a cooling rate of $\dot{\vartheta}$=2.5 K/s after deformation no bainite or martensite could be found in metallographic investigations (figure 2c1). Therefore, with the kind support of the Institut fuer Werkstoffkunde (IW) raster electron microscope (REM) analyses were used to get a closer look at the phase structure near to the indentations from hardness measurements (figure 2c2). As a result, a lamellar pearlitic structure with a comparatively high hardness H=486 HV (cf. table 2) was found. The shift of the pearlitic area for the samples of 100Cr6 due to previous deformation was also observed in the metallographic investigations. In the CCT-tests with the cooling rate $\dot{\vartheta}$=5 K/s and

φ=0, a purely martensitic microstructure was formed (figure 2d) whereas a in the tests with a previous forming a pearlitic-martensitic microstructure was generated (figure 2e). After calibration, the CCT-diagrams were converted to TTT-diagrams using the TTT-CCT-diagram generator.

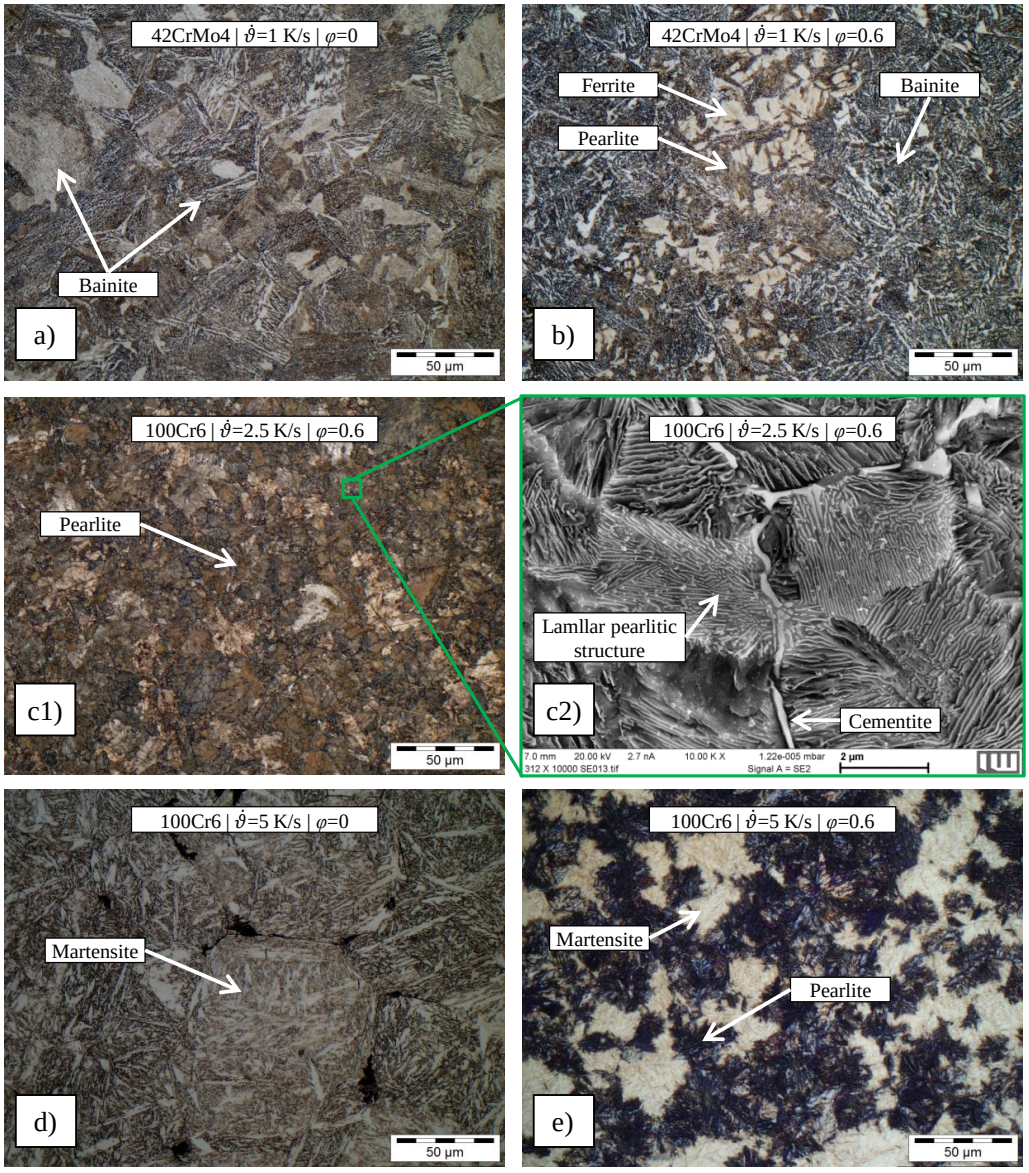

Figure 2: Microstructure of the specimens from 42CrMo4 after CCT-tests without (a) and with previous deformation (b); pearlitic phase of 100Cr6 after CCT-tests and previous deformation from metallographic (c1) and REM (c2) investigations; microstructure of the specimens from 100Cr6 after CCT-tests without (d) and with previous deformation (e).

2.2 Numerical determination of time temperature transformation diagrams

The determined TTT-diagrams were implemented in the commercial FE-software Simufact Forming 15 for numerical simulation of the CCT-tests. In order to reduce computational time rotationally symmetric 2D FE-simulations were carried out by exploiting the cylindrical shape of the specimens. The specimens have been discretised using a quad mesh with an element-edge-length of 0.05 mm. As initial configuration the thermally expanded geometry of the specimens at 950 °C with a completely austenitised structure was assumed. In the case of a CCT test with deformation, thermally conductive rigid punches with a quad mesh of 0.1 mm element-edge-length were used.

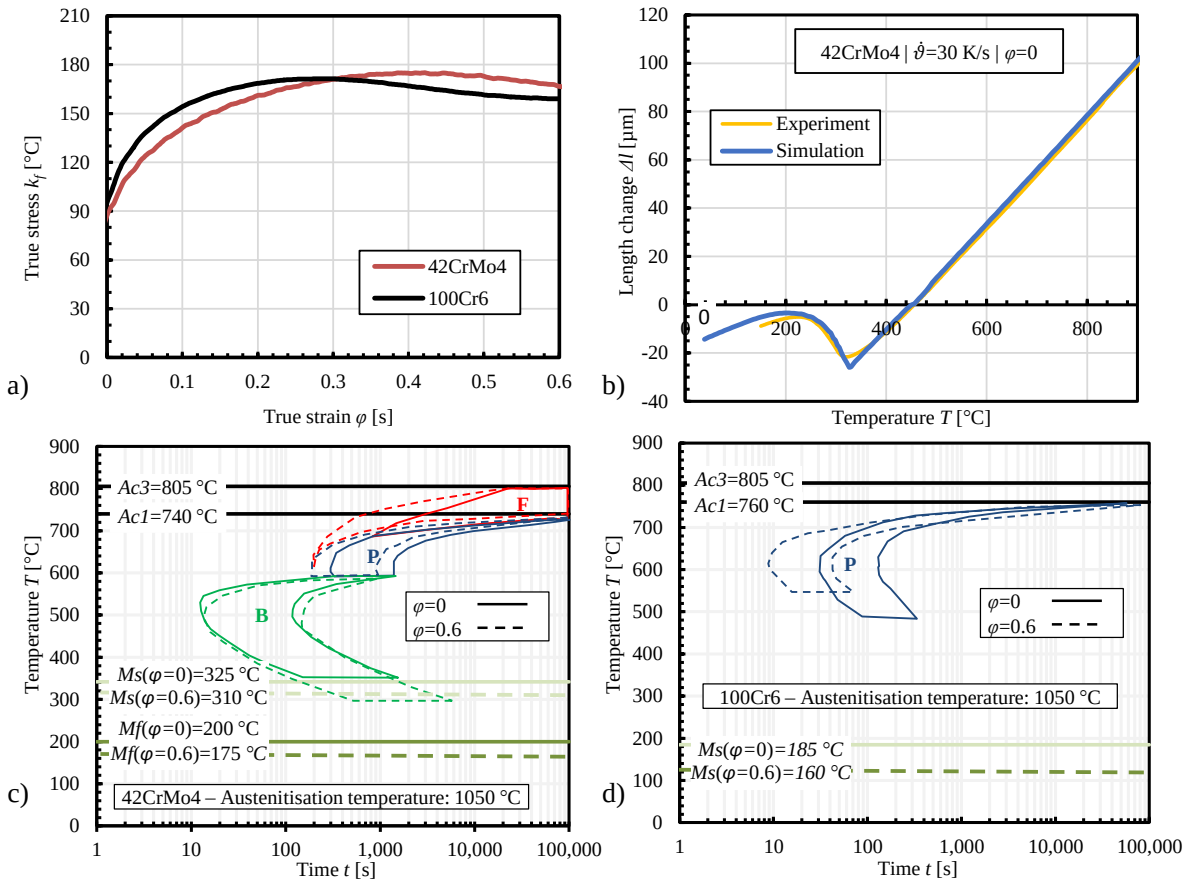

Figure 3: True stress k_f with respect to true strain φ of the investigated materials (a); comparison of experimentally measured and numerically calculated length-change Δl for the cooling rate $\dot{\vartheta}$ =30 K/s (b); TTT-diagrams with and without a previous deformation for the materials 42CrMo4 (c) and 100Cr6 (d).

The plastic deformation behaviour is described by flow curves at the relevant temperature 950 °C and the strain rate of 1 s^{-1} determined with help of the servohydraulic forming simulator Gleeble 3800-GTC from DSI company (figure 3a). As exemplarily illustrated in figure 3b the length-change Δl with respect to temperature T from the FE-simulations and the dilatometric CCT-experiments were compared. For further calibration, in an iterative procedure the TTT-diagrams were manually adjusted until the Δl-T profiles from experiment and simulation showed a good agreement. Additionally, the model was validated by a qualitative metallographic analysis of all experimentally tested specimens. Figure 3c and d show the finally determined TTT-diagrams for both materials with and without previous deformation.

3 Conclusion

In this study a cost-effective, time-saving as well as precise method for the determination of TTT-diagrams was presented for the steel alloys 42CrMo4 and 100Cr6. Initially CCT-diagrams were calculated with the software JMatPro of Sente Software based on the chemical composition of the steel alloys. These were optimised by experimental CCT-tests and subsequently converted into TTT-diagrams using the software tool "TTT-CCT-diagram generator" of Transvalor. The obtained TTT-diagrams were validated by a comparison of Δl from the FE-simulations and the dilatometric CCT-experiments as well as metallographic analyses. With this data in hand, phase transformation simulations aiming at subsequent residual stress calculation are possible.

Acknowledgement
Funded by the Deutsche Forschungsgemeinschaft (DFG, German Research Foundation) - 374871564 within the priority program SPP 2013.

References

[1] Verlinden B, Driver J, Samajdar J and Doherty RD (2007) Thermo-mechanical processing of metallic materials, Elsevier Science 11, ISBN: 9780080444970.
[2] Behrens BA and Olle P (2007) Consideration of phase transformations in numerical simulation of press hardening. Steel research international, 78(10-11), pp. 784-790.
[3] Behrens BA, Olle P, Schäffner C (2008) Process simulation of hot stamping in consideration of transformation-unduced stresses, Numisheet, Interlaken, Schweiz.
[4] Behrens BA, Bouguecha A, Bonk C, Chugreev A (2017) Numerical and experimental investigations of the anisotropic transformation strains during martensitic transformation in a low alloy Cr-Mo steel 42CrMo4, Procedia Engineering 207, pp. 1815-1820, ICTP2017, Cambridge, Great Britain.
[5] Doege E and Behrens BA (2016) Handbuch Umformtechnik, 3. Ed., Springer-Verlag, Berlin.
[6] Wever F, Rose A and Peter W (1961) Atlas zur Wärmebehandlung der Stähle Vol. 1 & Vol. 2, Verlag Stahleisen, Düsseldorf.
[7] Saunders N, Guo Z, Li X, Miodownik AP, Schillé JP (2004) The Calculation of TTT and CCT diagrams for General Steels.
[8] Kirkaldy JS and Venugopalan D (1983) Phase Transformations in Ferrous Alloys, D.A.R. Marder and J.I. Goldstein, eds., AIME, New York, NY, pp. 128-48.
[9] Li MV, Niebuhr DV, Meekisho LL, Atteridge DG (1997) A Computational Model for the Prediction of Steel Hardenability, Metall Mater Trans B, vol. 29, pp. 661-672.
[10] Schulze P, Schmidl E and Lampke T (2014) Entwicklung der Korngröße beim Erwärmen des Stahles 42CrMo4, WOMag (3).
[11] Nürnberger F, Grydin O, Schaper M, Bach FW, Koczurkiewicz B and Milenin A (2010) Steel Res. Int. 81, pp. 224-233.
[12] Behrens BA, Bouguecha A, Götze T, Moritz J, Sunderkötter C, Helmholz R and Schrödter J, (2013) Numerical and experimental analysis of the phase transformation during hot stamping process in consideration of strain-dependent CCT-diagrams, 4th International Conference on Hot Sheet Metal Forming of High-Performance Steel, Lulea, Sweden, pp. 329-336.
[13] Behrens BA, Schrödter J (2014) Numerical simulation of phase transformation during the hot stamping process, 5th International Conference on Thermal Process Modeling and Computer Simulation, Orlando, USA, S. 179-190.
[14] ASTM A1033 (2018) Standard Practice for Quantitative Measurement and Reporting of Hypoeutectoid Carbon and Low-Alloy Steel Phase, American Society for Metals, 2018.
[15] Yu Z, Gretzki T, Nürnberger F, Kästner M, Haskamp K, Bach F-W, Schaper M (2014) Wärmebehandlung, in Prozesskette Präzisionsschmieden, Bach F-W, Kerber K (Hrsg.), Springer-Verlag, Berlin Heidelberg, 2014.
Buza G, Hougardy HP, Gergely M (1990) Calculation of the isothermal transformation into two different microstructures from measurements with continuous cooling. Steel res 61(10), pp. 478–481.
[16] Rios PR (2005) Relationship between non-isothermal transformation curves and isothermal and non-isothermal kinetics. Acta Mater 53, pp. 4893–4901.
[17] DIN EN 10083-3 (2007) Steels for quenching and tempering – Part 3: Technical delivery conditions for alloy steels, Beuth-Verlag.
[18] DIN EN ISO 683-17 (2014) Heat-treated steels, alloy steels and free-cutting steels – Part 17: Ball and roller bearing steels, Beuth-Verlag.
[19] SEP 1680 (1990) STAHL-EISEN-Prüfblätter (SEP), 3rd Ed.
[20] SEP 1681, STAHL-EISEN-Prüfblätter (SEP), 2nd Ed., (1998).